Jurnal Polimesin
Department of Mechanical Engineering
State Polytechnic of Lhokseumawe
http://e-jurnal.pnl.ac.id/polimesin

e-ISSN	: 2549-1999	No.	: 3	Month	: June
p-ISSN	: 1693-5462	Volume	: 21	Year	: 2023

Article Processing Dates: Received on 2022-12-02, Reviewed on 2023-03-21, Revised on 2023-06-06, Accepted on 2023-06-07, and Available online on 2023-06-30

Analysis of intake air temperature effect on performance of portable atmospheric water generation (PAWG) systems with heat sink angle orientation of 75°

Muhamad Jafri*, Ben V. Tarigan, Hairman S. Lanae
Mechanical Engineering Department, Universitas Nusa Cendana, Kupang 85001,Indonesia
*Corresponding author: muhamad_jafri@staf.undana.ac.id

Abstract

The increasing demand for clean water and the diminishing supply of clean water sources can result in a clean water crisis. Air is a ubiquitous, inexpensive, and clean water source. Using Atmospheric Water Generators (AWG), the water contained in the air can be extracted. This study's objective was to determine the effect of inlet air temperature and air heater power variations on tool performance and PAWG condensate water production at a condenser angle of 75 degrees. The procedure utilized is experimental on three PAWG boxes. Each box has a distinct temperature at its entrance. The variation of inlet air temperature is accomplished by heating the air before it enters the box with an air heater; the applied power variations are 0.484 Watt, 0.964 Watt, and 1.702 Watt. The results demonstrated that variations in air heater power and inlet air temperature affected system performance and condensate water production. Maximum water discharge and PAWG performance were achieved when the air heating power was 0.48 watts and the water discharge was 1.166 milli liters per hour. At 0.0084 ml/h/W, the P_{Sys} system performance had the highest value. The variable air heating power of 0.946 Watt represents the utmost COP value of PAWG. This power variable has a high temperature difference and influences the COP value at high levels.

Keywords: Atmospheric air; thermoelectric; Peltier Element; PAWG; COP.

1 Introduction

All organisms require water for numerous processes and survival. Therefore, a sufficient water supply is required to meet water demands. The increasing demand for clean water and the decreasing supply of clean water could result in a water crisis. At least one month per year, two-thirds of the global population (4.0 billion people) experiences acute water scarcity [1]. Of course, some Indonesians also experience this. Initially, the earth was covered in water surfaces; however, as population pressure increases, the quantity of water surfaces is diminishing, and we must seek alternative water sources [2]. The atmosphere is an abundant, inexpensive, and pure source of water.

It is estimated that atmospheric air contains more than 12.91012 m^3 of renewable water, which is more than the total quantity of freshwater available in the world's marshes, wetlands, and rivers [3]. This quantity of water vapor is nearly 30 percent untapped water. Using or applying the Atmospheric Water Generators (AWG) tool [4] allows us to extract the water contained in atmospheric air. This AWG instrument can convert atmospheric air humidity directly into usable water, including potable water [5]. Humidity is the amount of water vapor in the air [6]. This term only applies to water in its gaseous state. There are numerous methods for analyzing humidity, including mixture ratio, specific humidity, and relative humidity. A portable atmospheric air water generator (Portable Atmospheric Water Generators) PAWG, which is smaller in size, lighter in weight, and uses less energy, is presently being developed as one of the tools for producing water from atmospheric air [7]. The thermoelectric cooling (TEC) module serves a crucial role in converting atmospheric air into water in the PAWG.

A thermoelectrical module is a device that, when subjected to a direct electrical voltage, can generate a temperature difference. Thermoelectric cooling (TEC) technology, which utilizes the Peltier effect to generate a heat flux between the junction of two distinct types of materials, has attracted widespread interest over the past few decades. When the Peltier element is supplied with DC electrical energy in a pair of P-type semiconductor cells (which have a low energy level), thermoelectric cooling based on the Peltier effect is initiated. The higher energy level of the N-type semiconductor will cause one side of the Peltier element to cool (heat absorption process) and the other side to heat [8]. To calculate the dew point temperature from [9], the location must know the current air temperature and relative humidity. For 100 percent relative humidity, the dew point temperature is the same as the atmospheric temperature.

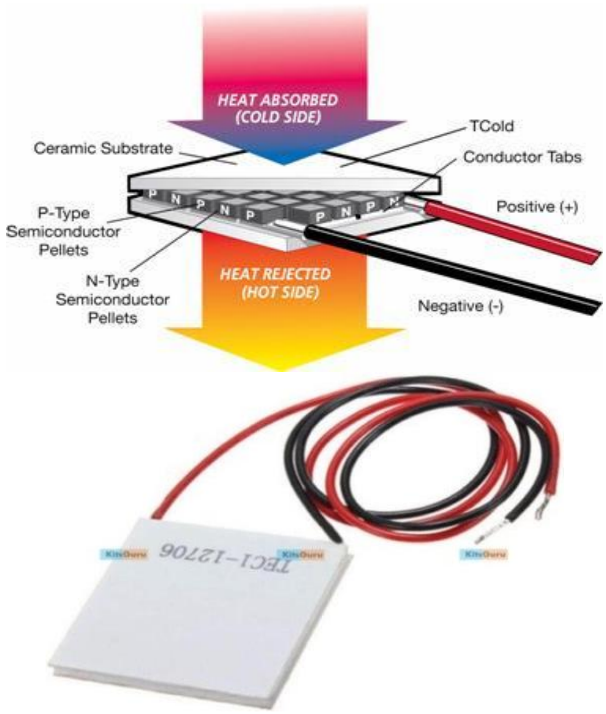

Fig. 1. Peltier Element [10].

COP investigations of TEC modules, which examined materials with modelling approaches, and strategies to improve cooling performance [11] and [7], using genetic algorithms to optimise thermoelectric coolers in limited volumes [12].

In addition to the thermoelectric module, there is a fan that provides the necessary airflow and moves air into the heatsink to aid in the condensation process. Condensation is the physical transformation of vapour from the vapor phase to the liquid phase.

Humidity is the quantity of water vapor that the air can hold. Air humidity can provide a remedy for the dearth of potable water. Because the atmosphere contains an estimated 12.9 1012 m3 of regenerative water. Temperature determines the maximum quantity of water vapor present in the air. Warm air is capable of holding more water vapor than frigid air [4]. Designed a heat sink with rectangular fins and analyzed the influence of various operational parameters, including heat sink spacing with/without fan, fan voltage, and heat applied to the heat sink [13]. [14] When designing microchannel heat sinks that use water or air as a coolant to dissipate heat. Experiments indicate that the orientation of the thermoelectric condenser should be considered in order to optimize the water collection rate under high humidity conditions [15].

This AWG device employs latent heat to transform molecules of water vapor into water droplets. Similarly, a PAWG (portable air water generator) is a tiny, simple AWG that can be transported and only produces a small quantity of condensate water. The temperature required for water to condense is known as the dew point temperature. Before selecting an efficient device, several parameters must be determined, including cold surface temperature (TC) and heated surface temperature (TH). TH incorporates two primary parameters, the first of which is the device's efficiency, which is the difference between the device's hot surface temperature and the ambient temperature. Second, the temperature of the environment in which the heat dissipates [5]. The cold surface temperature (TC) and the heated surface temperature (TH) are determined by the air temperature entering the PAWG system.

Each location simultaneously enters the system at a distinct ambient temperature. Low, moderate, high, and even extreme temperatures exist. The quantity of water vapor in the air increases as the temperature rises. Consequently, muggy and humid environments contain more water vapor [16]. In previous studies, variations in the orientation of the condenser angle were observed, but not the effect of air temperature entering the box if the temperature of the incoming air varied at each location. Therefore, it is necessary to conduct research representing a range of low to high environmental temperatures. Obtaining an inlet air temperature that varies from low to high at a particular location is challenging, so adjusting the power variation on the air heater installed on the inlet side of the system will cause inlet air temperature variations.

This research seeks to determine the impact of inlet air temperature and air heater power variations on the system performance and condensate water production of PAWG with a heatsink angle of 750 degrees. The angle orientation of heatsinks is based on previous research [17]. The experimental research procedure employs three PAWG boxes, each of which has a different temperature. The variation of inlet air temperature is accomplished by heating the air before it enters the box with an air heater of varying power, specifically 0.484 Watt, 0.964 Watt, and 1.702 Watt.

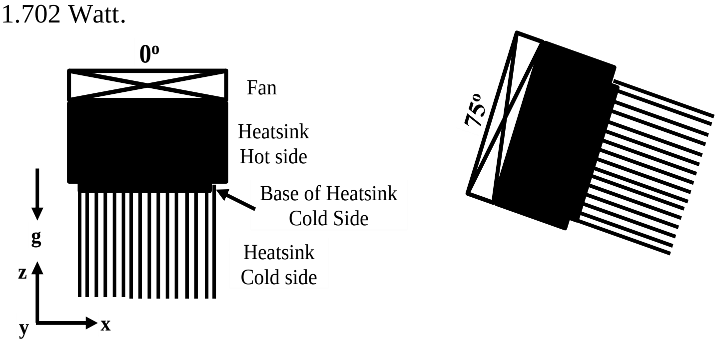

Fig. 2. Orientation of Heatsink 75^{O}

2 Research Methods

This research was conducted at the Mechanical Engineering Laboratory of Nusa Cendana University from 08:00 AM on 23 June 2022 until 08:00 AM on 24 June 2022. The tools and materials used in this research are;

Table 1. Tools and materials used in this research.

Material/Tools Name	Specifications
	Tools
Power supply	*12V 40A Switching Trafo Jaring*
Fan	Item Dimensions: 24x12,5x6,5cm
Peltier Element	*Brand Name* : *Generic,* EAN : 6329161934776, *Item Wight* : 20.0 grams, *Manufacturer Series Number* : KG103
Inlet Fan	*Size* : 12*12*1.3cm, *Fan interface* : 2.0 2 pin, *Voltage* : AC12V±20%, *Rotate speed* : 3000 rpm±15%, *Wire Length* : 10cm)
Hot side heatsink Fan	*Size* : 9*9*2.5cm, *Current* : 0.30A, *Rotate speed* : 2500 rpm, *Frequency* : 50/60Hz, *Voltage* : DC 12V
Air heater 220°C	*Size* : 2*3*0.5cm, Power : 1-30 w, Voltage DC 12 V
Measuring Cup	*Volume capacity : 0-120 ml*
Hot Wire Anemometer	*SKU KW0600653*
	Materials
Outer Heatsink	*Length : 10cm, Number of fins : 21*
Inner Heatsink	*Length : 4 cm, Number of fins: 8*
Acrylic	*Thick 2 mm*

The PAWG tool shown in Fig. 3.

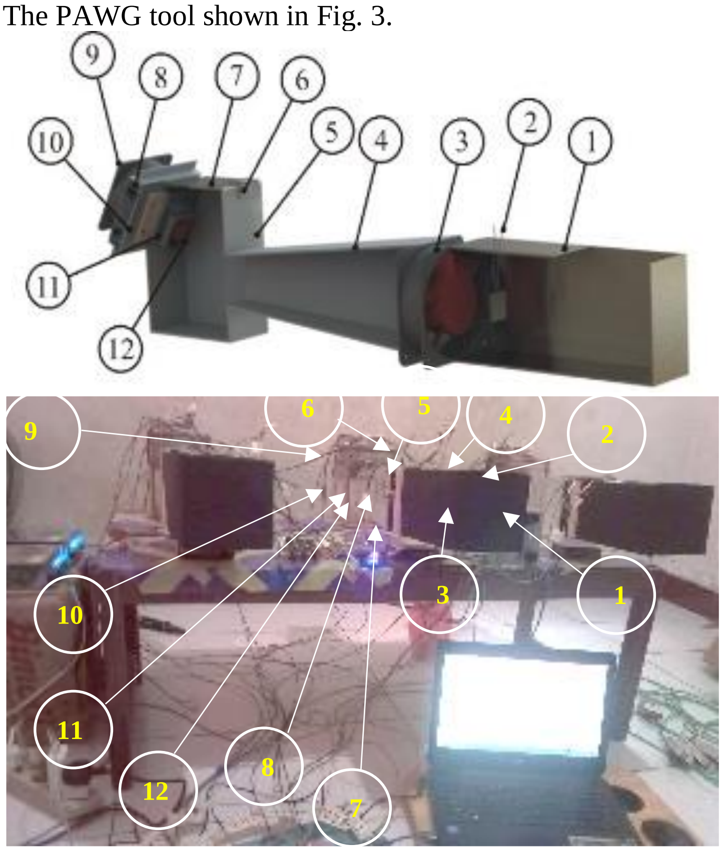

Description: 1. Inlet air box, 2. Air heater, 3. Inlet air fan, 4. Inlet air funnel, 5. Condensation chamber, 6. Hinge, 7. Portable converter cover, 8. Hot heatsink, 9. Hot side heatsink fan, 10. Peltier, 11. Cold heatsink, 12. Cold side heatsink fan.

Fig. 3:. Schematic of the PAWG tool system

The operating principle of this device is that ambient air enters through the inlet and passes through the air heater to reach the desired temperature. By using a fan, the compartment is filled with air. This process can be accelerated by passing the same hot air through the cold side of the TEC so that the water droplets do not freeze and water condensation occurs.

The data was collected by situating temperature measuring instruments on the inlet side, within the box, on the cold side of the Peltier, on the hot side of the Peltier, and at the ambient temperature. This study measured the temperature inside the box, the cold side Peltier temperature, the hot side Peltier temperature, the inlet air temperature, and the environmental temperature using a thermocouple data recorder and the Elitech-RC-4Hac to measure the outside and inside humidity. These data are calculated in real-time using a data recorder, and freshwater production data is measured with a measuring cup.

The research commences with the placement of three PAWG test media representing three independent variables, namely the inlet air temperature heated by an air heater with 0.484 Watt, 0.964 Watt, and 1.702 Watt of power. While the dependent variable is the PAWG tool's performance. The three media were set in an open area with a northern orientation. Using temperature data loggers, thermocouple data loggers, and outside and inside humidity sensors, they calibrate measuring instruments. Every two hours for 24 hours, beginning at 08.00 WIB and ending at 08.00 WIB the following day, data is collected. Before testing, all testing instruments must undergo the calibration procedure.

The measurement data were tabulated to generate a graph illustrating the relationship between the test variables and each independent variable. In addition, the data were processed with formulas in order to ascertain the performance of the PAWG system via COP (coefficient of performance) analysis and developed performance analysis. To evaluate the performance of the PAWG system, one can use the formula devised in [17].

$$P_{Sys} = \frac{W_{g/hour}}{P_{AWG}} \tag{1}$$

Where P_{Sys} is the system performance, Wg/hour is the flow rate of water produced in (ml/h), while PAWG is the sum of the power consumed by the incoming fan (P_{Fan1}), the energy consumed by the outgoing fan (P_{Fan2}) and the power consumed by the Peltier ($P_{Pel.}$);

$$P_{AWG} = P_{Fan,1} + P_{Fan,2} + P_{Pel.} \tag{2}$$

3 Results and Discussion.

3.1 Results

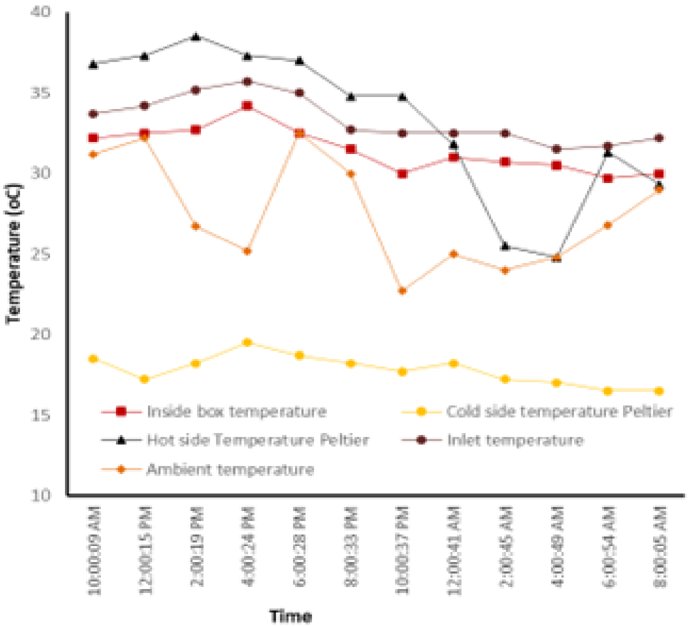

(a)

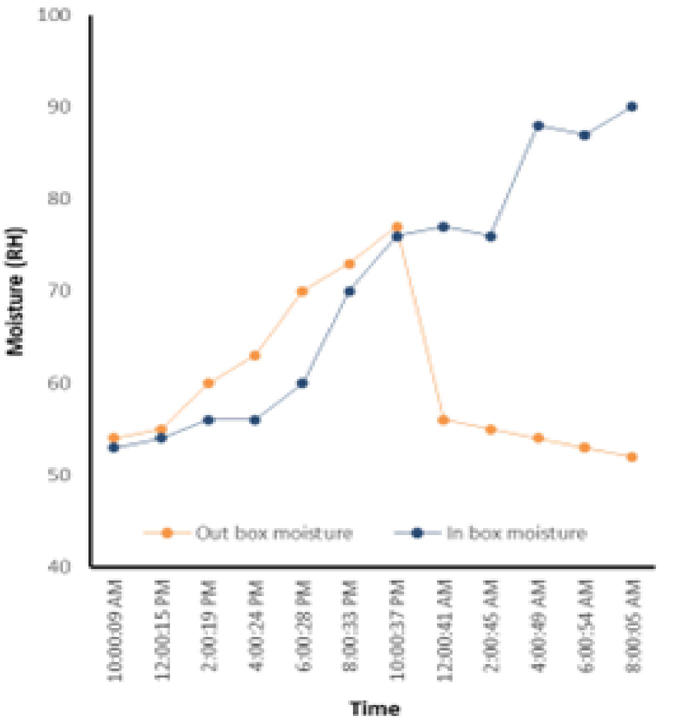

(b)

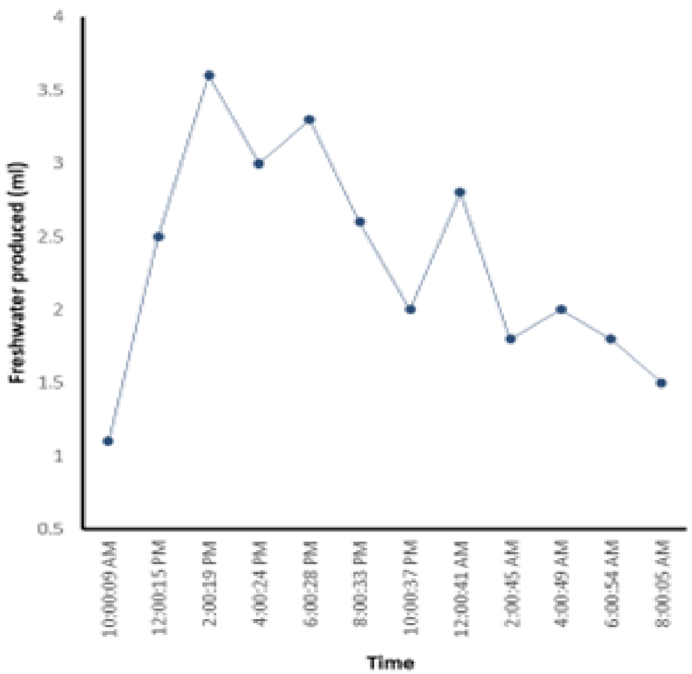

(c)

Fig. 4. Graph of the relationship between temperature, humidity and volume of water produced by the heater variation with a power of 0.484 Watt. (a) Temperature vs Time, (b) Moisture vs Time, (c) Freshwater produced vs Time.

The results of testing the effect of changes in inlet air temperature through variations in heater power of 0.484 Watts, 0.946 Watt, and 1.702 Watt on water productivity are tabulated and graphed as shown in the following Fig. 4.

With an inlet air velocity of 0.97 m/s and a heating power of 0.484 Watt, as shown in Fig. 4, the temperature of the hot side Peltier is the highest, followed by the temperature in the box and the ambient temperature, and the temperature of the cool side Peltier is the lowest. At 2:19 p.m., the Peltier hot side temperature reached its maximum point of 38.5oC, before dropping to 24.8ºC. The cold side of the Peltier reached its maximum temperature of 19.5ºC at 4:24 a.m. and then dropped to 16.5ºC. The relative humidity inside the PAWG instrument reduced at the beginning of the test and then increased to 90%, whereas the relative humidity outside grew from the beginning to the middle of the test and then decreased. While the highest freshwater productivity occurred at 2:19 PM, at 3.6 ml, and the lowest at 10:09 AM, at 1.1 ml, the lowest freshwater productivity occurred at 10:09 AM, at 1.1 ml.

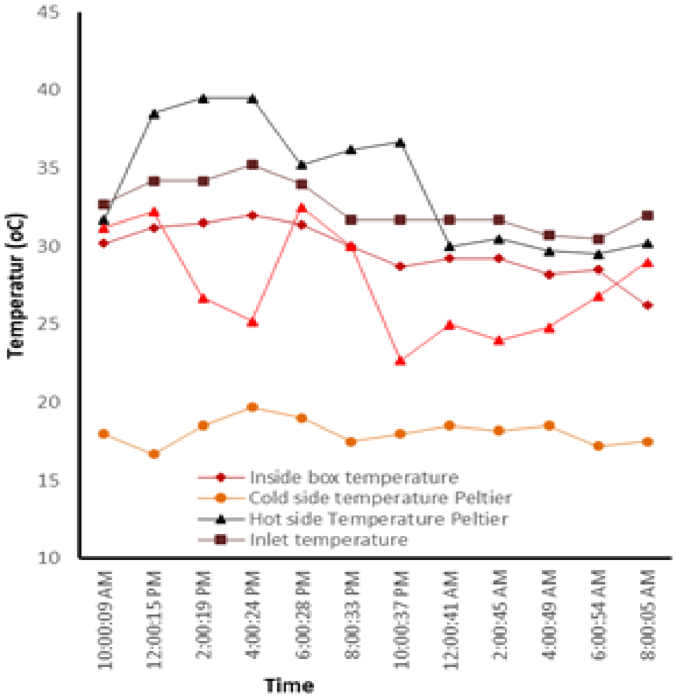

(a)

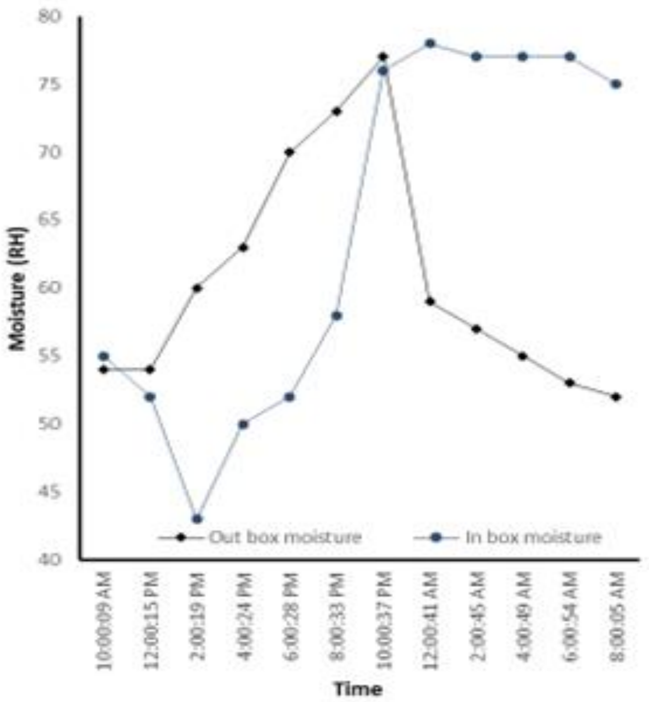

(b)

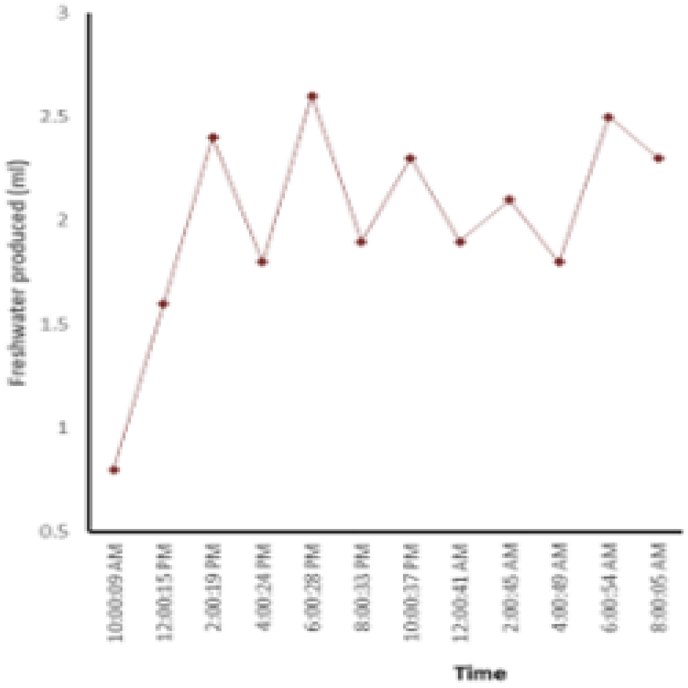

(c)

Fig. 5. Graph of the relationship between temperature, humidity and volume of water produced by the heater variation with a power of 0.946 watts. (a) Temperature vs Time, (b) Moisture vs Time, (c) Freshwater produced vs Time.

For PAWG with an air velocity of 0.97 m/s and heating power of 0.946 watts (Fig. 5), the highest Peltier hot-side temperature occurred at 2:19 PM at 39.5ºC, then decreased to 29.5ºC. While the Peltier cold side temperature, the highest temperature occurred at 4:24 PM, which was 19.7ºC and dropped to 16.7ºC. The humidity in the PAWG device initially decreased at the beginning of the test and then increased to 78%, while the outside humidity, from the beginning to the middle of the test time, increased and then decreased. The highest freshwater productivity occurred at 6:28 PM at 2.6 ml, and the lowest occurred at 10:09 AM with a water production of 0.8 ml.

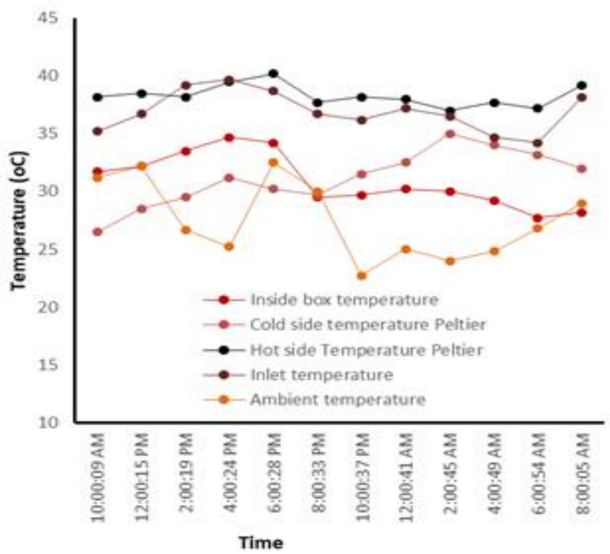

(a)

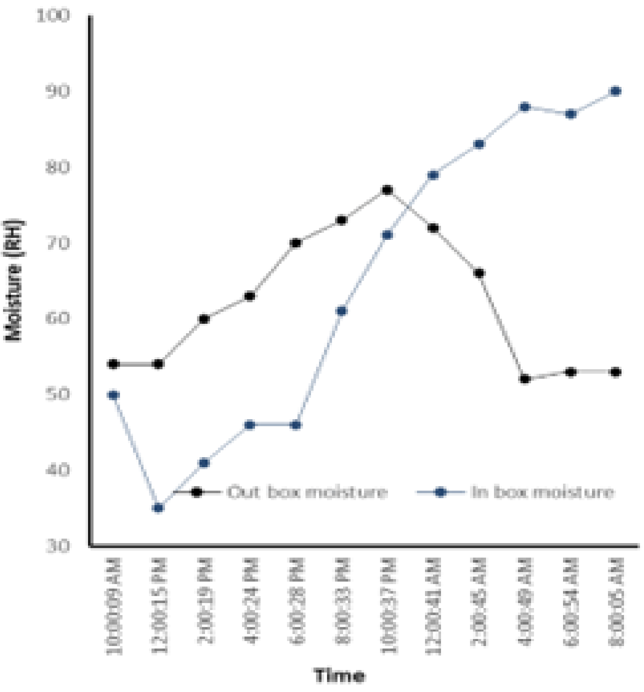

(b)

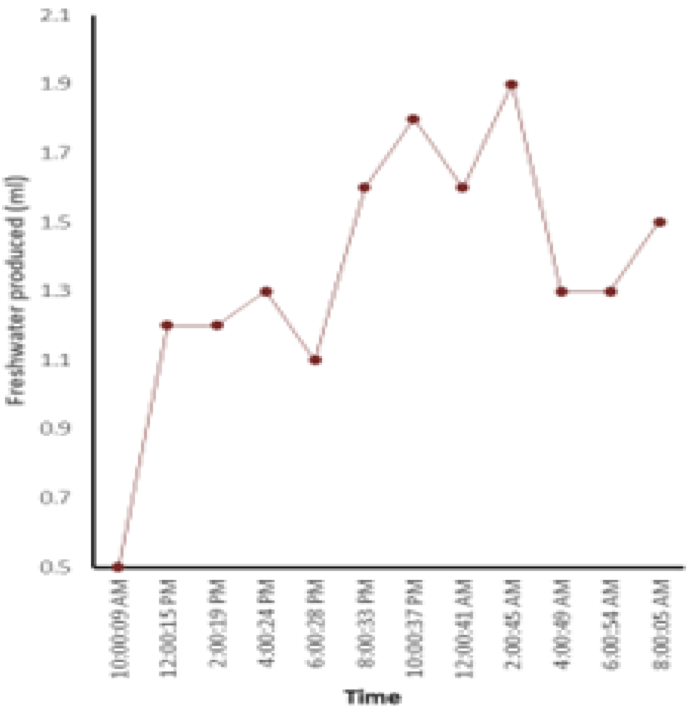

(c)

Fig. 6. Graph of the relationship between temperature, humidity and volume of water produced by the heater variation with a power of 1,702 Watts. (a) Temperature vs Time, (b) Moisture vs Time, (c) Freshwater produced vs Time..

As for the PAWG with an air velocity of 0.97 m/s and heating power of 1,702 Watt (Fig. 6), for each time the data is taken, the Peltier hot side temperature is the highest, followed by the temperature in the box, environmental temperature, and the lowest Peltier cold side temperature. The highest Peltier hot-side temperature occurred at 06:28 PM at 40.2°C, then decreased to 37°C. Peltier cold side temperature, the highest temperature, occurred at 02:45 AM, which was 35ºC and decreased to 26.5ºC. The humidity inside the PAWG device initially reduced at the beginning of the test and then increased to 88%, while the outside humidity, from the beginning to the middle of the test time, rose and then decreased. The highest freshwater productivity occurred at 2:45 AM at 1.9 ml, and the lowest freshwater production occurred at 10:09 AM with a water production of 0.5 ml.

3.2 Research Data Processing

The data processed in this study are fan specification data such as Peltier elements. This data is processed using formulas to obtain system performance and the system's Coefficient of Performance. To analyse the performance of the PAWG system, equations (1) and (2) can be used.

The results of the data analysis of the PAWG system performance, namely $P_{Sys.}$ They are tabulated, as shown in Table 1 and made as a graph in Fig. 6 to facilitate discussion.

Table 2. The results of the system performance analysis (PAWG) are $P_{Sys.}$ for heater variations with power of 0.484 Watts, 0.946 Watts, and 1.702 Watts.

Heater Variety	Wg/hour (ml/h)	PAWG (Watt)	P_{sys} (ml/h/W)
Box 1 (0.484 watt)	1.166	137.4	0.0849
Box 2 (0.946 watt)	1.000	137.4	0.0727
Box 3 (1.702 watt)	0.675	137.4	0.0491

The table 2 shown in graph form as shown in Fig. 6.

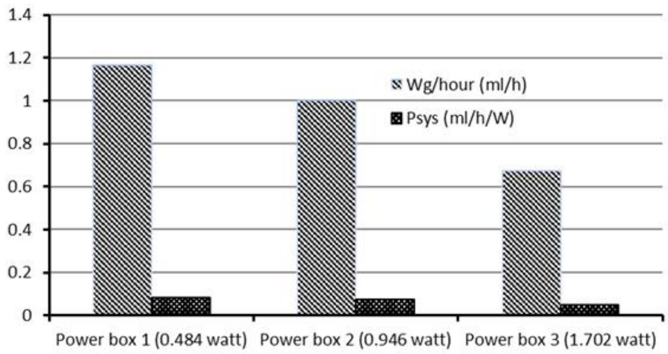

Fig. 6. Relationship between heating variation and P_{Sys}

The performance of a PAWG device is assessed by the magnitude of the Coefficient of Performance (COP) [18] with Eq. 3:

$$COP = \frac{Ouput}{Input} \tag{3}$$

The output or goal of the PAWG system is the condensation effect, while the input effect is the energy absorbed by the Peltier and fan. So Eq. 3 becomes Eq. 4;

$$COP = \frac{\text{Condensation effect}}{\text{Pin}} \tag{4}$$

COP is the heat absorbed on the cold side Qc divided by the input power: COP = Qc/P_{in} [19]. So in this study, Qc is the condensation effect while P_{in} is $P_{Fan} + P_{Peltier}$ (Eq. 5-6).

$$COP = \frac{Qc}{P_{in}} = \frac{Qc}{P_{Fan} + P_{Petier}} \tag{5}$$

where;

$$Qc = \dot{m}(h_{Hot} - h_{Cold}) \tag{6}$$

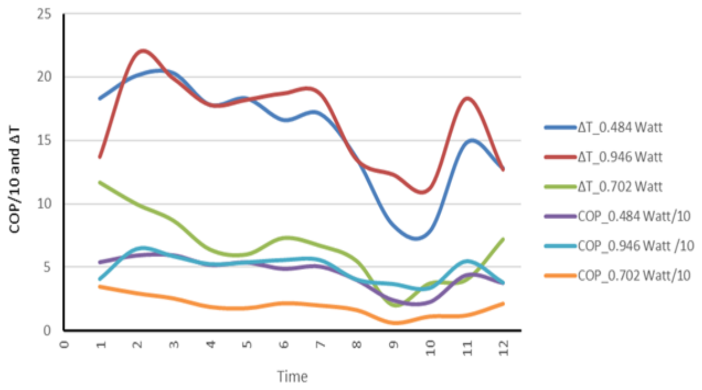

Fig. 7. Relationship between independent variables on COP and ΔT

3.3 Discussion

Peltier hot side and Peltier cold side temperature changes for 0.484 Watt, 0.946 Watt, and 1.702 Watt water heater power exhibit the same trend of change from 10:09 a.m. to 10:37 p.m., but then decrease slightly for Peltier cold side temperature and increase slightly for Peltier hot side temperature until the conclusion of the test. The decreasing temperature trend of the Peltier's hot side and cold side at the conclusion of the test is directly proportional to the decreasing outside humidity. Obviously, the temperature of the heated side of the Peltier and the cold side of the Peltier is affected not only by the temperature of the air passing through the air heater, but also by the surrounding humidity. This result explains why the cold side surface temperature drops below the dew point of the incoming humid air temperature, resulting in the formation of a water deposit on the cold side surface. As a consequence, heat and mass transfer occur simultaneously near the surface of the cold side, and both heat transfer processes are mutually advantageous. Increasing the relative humidity of incoming moist air contributes to mass transfer as the moisture content difference between incoming air and air near the frigid surface increases. A more efficient mass transfer accelerates heat transfer from the inlet air to the cold-side surface, so the temperature of the cold-side surface rises as the relative humidity of the inlet air rises. The same trend occurs in the surface temperature of the hot side and is associated with an increase in heat transfer from the cold side to the heated side.

Fig. 6. depicts the water discharge produced by each variable water heater, with the 0.484 Watt water heater discharging 1.16666 ml/hour and the P_{Sys} system discharging 0.00849 ml/h/w. For the air heater, 0.946 Watt decreased to 1.0 ml/hour, followed by a 0.00728 ml/h/w decrease in P_{Sys} system performance. But for the 1.702 Watt water heater, the water discharge is reduced to 0.67 ml/hour, followed by a 0.0041 ml/h/w decrease in P_{Sys} system efficacy. The heating variation with 0.484 watts results in the greatest water discharge and the highest system performance; this is because the small power causes low inlet air temperature, which, when in contact with the constant cold and hot side heat sink, produces a great deal of water and maximum performance.

Fig. 7 reveals that the variable air heater with a COP of 0.946 Watt has the highest COP, followed by the variable air heater with a COP of 0.484 Watt, and the variable air heater with a COP of 1.702 Watt has the lowest COP. This occurs due to the temperature difference (T) between the hot side and cool side of the Peltier device. As can be seen in the graph, the greater the temperature difference, the greater the COP. Maximum temperature difference (T) is observed in the variable air heater at 0.946 watts, followed by the variable air heater at 0.484 watts and the variable air heater at 1.702 watts with the lowest COP. This occurs because, with sufficient power to generate high inlet air temperatures, the water vapor produced by latent heat is suboptimal.

4 Conclusions.

The conclusion that can be derived is that the water discharge generated by each variable water heater is 1.16666 ml/hour for the 0.484 Watt water heater and 0.00849 ml/h/day for the P_{Sys} system. For the air heater, 0.946 Watt decreased to 1.0 ml/hour, followed by a 0.00728 ml/h/w decrease in P_{Sys} system performance. But for the 1,702 Watt water heater, the water discharge is reduced to 0.67 ml/hour, followed by a 0.0041 ml/h/w decrease in P_{Sys} system efficacy. The 0.484 Watt heater variation produces the highest water discharge and has the highest system performance of the three variations listed above. The COP indicates the efficacy of the PAWG, with the variable water heater having the highest COP at 0.946 watts. As can be seen in the graph, the greater the temperature difference, the greater the COP. It comes out that the variable air heater has the greatest temperature difference (T) at 0.946 watts..

References.

[1] D. Subhan, U. M. Tang, and F. Fatnanta, “Strategi Pemanfaatan Sumber Air Di Kabupaten Siak Untuk Pengembangan Unit Pelayanan Teknis Daerah (Uptd) Air Minum Kabupaten Siak,” *Phot. J. Sain dan Kesehat.*, vol. 7, no. 01, pp. 11–18, 2016, doi: 10.37859/jp.v7i01.554.

[2] M. Sajid, I. Hassan, and A. Rahman, “An overview of cooling of thermoelectric devices,” *Renew. Sustain. Energy Rev.*, vol. 78, pp. 15–22, 2017, doi: https://doi.org/10.1016/j.rser.2017.04.098.

[3] G. M. Peters, N. J. Blackburn, and M. Armedion, “Environmental assessment of air to water machines - Triangulation to manage scope uncertainty,” *Int. J. Life Cycle Assess.*, vol. 18, no. 5, pp. 1149–1157, 2013, doi: 10.1007/s11367-013-0568-2.

[4] D. Milani, A. Qadir, A. Vassallo, M. Chiesa, and A. Abbas, “Experimentally validated model for atmospheric water generation using a solar assisted desiccant dehumidification system,” *Energy Build.*, vol. 77, pp. 236–246, 2014, doi: 10.1016/j.enbuild.2014.03.041.

[5] A. Nandy, S. Saha, S. Ganguly, and S. Chattopadhyay, “A Project on Atmospheric Water Generator with the Concept of Peltier Effect,” *Int. J. Adv. Comput. Res.*, no. 2, pp. 2277–7970, 2014.

[6] Chakib Alaoui, “Peltier thermoelectric modules modeling and evaluation,” *Int. J. Eng*, no. 5, pp. 114–121, 2011.

[7] S. Liu *et al.*, “Experimental analysis of a portable atmospheric water generator by thermoelectric cooling method,” *Energy Procedia*, vol. 142, pp. 1609–1614, 2017, doi: 10.1016/j.egypro.2017.12.538.

[8] Mangsur, “Pengembangan cool tipe CB-02 Multifungsi Ramah Lingkungan Berbasis Termoelektrik untuk Kendaraan Roda Dua,” Universitas Indonesia, Depok, 2010.

[9] M. Eslami, F. Tajeddini, and N. Etaati, “Thermal analysis and optimization of a system for water harvesting from humid air using thermoelectric coolers,” *Energy Convers. Manag.*, vol. 174, no. March 2019, pp. 417–429, 2018, doi: 10.1016/j.enconman.2018.08.045.

[10] https://www.amazon.in/Generic-Thermoelectric-Peltier-Cooler%20Cooling/dp/B00YUP56NC?th=1, “Industrial and Scientific.”

[11] W. He, P. Yu, Z. Hu, S. Lv, M. Qin, and C. Yu, “Experimental study and performance analysis of a portable atmospheric water generator,” *Energies*, vol. 13, no. 1, pp.

1–14, 2019, doi: 10.3390/en13010073.
[12] Y.-H. Cheng and W.-K. Lin, "Geometric optimization of thermoelectric coolers in a confined volume using genetic algorithms," *Appl. Therm. Eng.*, vol. 25, no. 17–18, pp. 2983–2997, Dec. 2005, doi: 10.1016/j.applthermaleng.2005.03.007.
[13] C. Udomsakdigool, J. Hirunlabh, J. Khedari, and B. Zeghmati, "Design Optimization of a New Hot Heat Sink with a Rectangular Fin Array for Thermoelectric Dehumidifiers," *Heat Transf. Eng.*, vol. 28, no. 7, pp. 645–655, Jul. 2007, doi: 10.1080/01457630701266470.
[14] R. Chein and G. Huang, "Thermoelectric cooler application in electronic cooling," *Appl. Therm. Eng.*, vol. 24, no. 14–15, pp. 2207–2217, 2004, doi: https://doi.org/10.1016/j.applthermaleng.2004.03.001.
[15] C. T. Hand and S. Peuker, "An experimental study of the influence of orientation on water condensation of a thermoelectric cooling heatsink," *Heliyon*, vol. 5, no. 10. 2019. doi: 10.1016/j.heliyon.2019.e02752.
[16] I. Lekouch *et al.*, "Influence of temporal variations and climatic conditions on the physical and chemical characteristics of dew and rain in South-West Morocco," *5th Int. Conf. Fog, Fog Collect. dew*, no. July, pp. 4–7, 2010.
[17] I. Casallas, M. Pérez, A. Fajardo, and C. I. Paez-Rueda, "Experimental parameter tuning of a portable water generator system based on a thermoelectric cooler," *Electron.*, vol. 10, no. 2, pp. 1–14, 2021, doi: 10.3390/electronics10020141.
[18] Y. A. Çengel and M. A. Boles, *Thermodynamics: An Engineering Approach*, 5th ed. Michigan: McGraw-Hill Higher Education, 2007.
[19] M. E. GmbH, "https://www.meerstetter.ch/customer-center/compendium/70-peltier-elements#COP."